ISSN : 0974 - 7524 Volume 7 Issue 4

Physical CHEMISTRY
An Indian Journal

Trade Science Inc.

Full Paper

PCAIJ, 7(4), 2012 [117-128]

Kinetics study of the reaction between triphenylphosphine, dialkyl acetylenedicarboxylates and 2-mercaptobenzimidazole along with theoretical calculations: A mechanistic investigation

Mohammad Zakarianezhad[1], Hojjat Ghasempour[2], Sayyed Mostafa Habibi Khorassani[3,*], Malek Taher Maghsoodlou[3]

[1]Department of Chemistry, Payam Noor University, Tehran, (IRAN)
[2]Department of Chemistry, Bardsir Branch, Islamic Azad University, Bardsir, (IRAN)
[3]Department of Chemistry, The University of Sistan and Baluchestan, Zahedan, (IRAN)
E-mail: habibi_khorassani@yahoo.com

Received: 21st January, 2012 ; Accepted: 21st February, 2012

ABSTRACT

In the recent work, stability of the *Z*- and the *E*- isomers were undertaken for the two rotational isomers of phosphorus ylides involving a 2-mercaptobenzimidazole [namely dimethyl 2-(2-mercaptobenzimidazole-s-yl)-3-(triphenylphosphanylidene) succinate] by natural population analysis (NPA) and atoms in molecules (AIM) methods. Quantum mechanical calculation was clarified how the ylides exist in solution as a mixture of the two geometrical isomers (*Z*- and *E*-) as a major or minor form. In addition, kinetic studies were performed for the reaction between triphenylphosphine, dialkyl acetylenedicarboxilate in the presence of SH-acid, such as 2-mercaptobenzimidazole by UV spectrophotometery technique. The values of the second order rate constant (k_2) were calculated using standard equations within the program. All reactions repeated at different temperature range, the dependence of the second order rate constant with temperature was in a good agreement with Arrhenius and Eyring equations. This provided the relevant plots to calculate the activation parameters (ΔH#, ΔS# and ΔG#) of all reactions. Furthermore useful information was obtained from studies of the effect of solvent and concentration of reactants on the rate of reaction. Proposed mechanism was confirmed according to the obtained results and steady state approximation and first step (k_2) of reaction was recognized as a rate determining step on the basis of experimental data.

KEYWORDS

Kinetic study;
UV spectrophotometery;
Z and *E* rotamers;
Stable phosphorus ylides.

INTRODUCTION

Organophosphorus compounds have emerged as important reagents and intermediates in organic synthesis[1]. An important group of this class is phosphorus ylides, which have been used in many reactions and synthesis of organic compounds[2-29]. The prominent role of these compounds is to convert the carbonyl groups

to carbon-carbon double bonds[10] from the large number of methods available for the synthesis of phosphorus ylides, the most important involve the reaction of a phosphonium salt with a base[12,25]. In recent years a method has been developed for the preparation of this family by using a novel approach employing vinyl phosphonium salts[16,21]. The phosphonium salts are most often converted to the ylides by treatment with a strong base, though weaker bases can be used if the salt is acidic enough. Michael addition of phosphorus (III) compounds such as triphenylphosphine to acetylenic esters leads to reactive 1, 3-dipolar intermediate betaines which are not detected even at low temperature[23]. These unstable species can be trapped by a protic reagent, ZH, such as methanol, amide, imide, etc. to produce various compounds e.g. ylides[5-29].

These ylides usually exist as a mixture of the two geometrical isomers, although some ylides exhibit one geometrical isomer. Assignment of the stability of the two *Z*- and *E*- isomers is impossible in phosphorus ylides by experimental methods such as ^{1}H and ^{13}C NMR and IR spectroscopes, mass spectrometry and elemental analysis data. For this reason quantum mechanical calculation has been performed in order to gain a better understanding of the most important geometrical parameters and also relative energies of both the geometrical isomers.

MATERIAL AND METHODS

Quantum mechanical calculation has been performed by Gaussian98 program and using the AIM2000 program packages. dialkyl acetylenedicarboxilate, triphenylphosphine and 2-mercaptobenzimidazole were purchased from Fulka (Buchs, Switzerland) and used without further purification. All extra pure solvents including 1, 2-dichloroethane and ethyl acetate also obtained from Merk (Darmstadt, Germany). A Cary UV/Vis spectrophotometer model Bio-300 with a quartz cell with 10 mm light-path was employed throughout the current work.

RESULTS AND DISCUSSION

Calculations

A facile synthesis of the reaction between triphenylphosphine 1, dialkyl acetylendicarboxylates 2 and 2-mercaptobenzimidazole 3 (as a SH- heterocyclic compound) for generation of phosphorus ylides 4a-b involving the two geometrical isomers such as *Z* and *E* isomers have been earlier reported[30]. The reaction is shown in Figure 1. For assignment of the two *Z* and *E* isomers as a minor or major form in phosphorus ylides 4a-b containing a 2-mercaptobenzimidazole, first the *Z*- and the *E*- isomers were optimized for all ylide structures at HF/6-31G(d,p) level of theory by Gaussian98 package program[31]. The relative stabilization energies in both the geometrical isomers have been calculated at HF/6-31G(d,p) and B3LYP/6-311++G(d,p) levels. Atoms in molecules (AIM)[32], natural population analysis (NPA) methods and CHelpG keyword at HF/6-31G(d,p) level of theory have been employed in order to

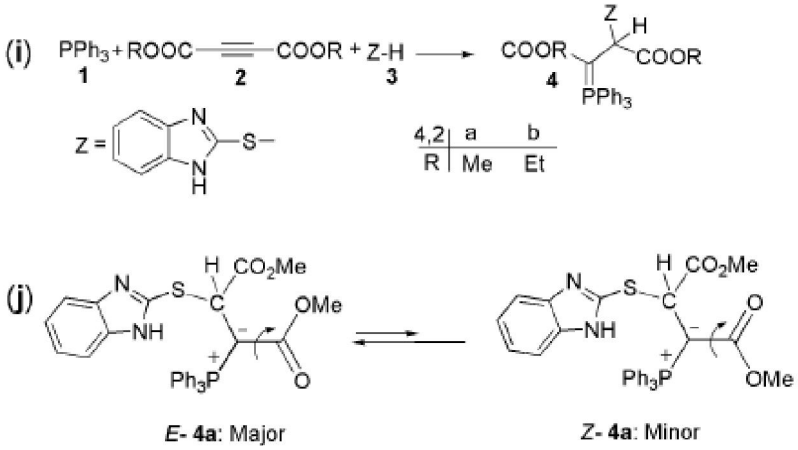

Figure 1 : (i) The reaction between triphenylphosphine 1, dialkyl acetylenedicarboxylate 2 (2a or 2b) and 2-mercaptobenzimidazole 3 for generation of stable phosphorus ylides 4 (4a or 4b). (j) The two rotational of isomers *Z*-4a and *E*-4a (minor and major, respectively) for ylide 4a.

gain a better understanding of most geometrical parameters of both the *E*-4(a, b) and the *Z*-4(a, b) of phosphorus ylides. The numbers of critical points and intramolecular hydrogen bonds as well as the charge of atoms that constructed on the *Z*- and *E*- isomers have been recognized. The results altogether reveal the effective factors on stability of *Z*- and *E*- ylide isomers. The relative stabilization energies for the two [*Z*-4(a, b) and *E*-4(a, b)] isomers (See Figures 2 and 3) are reported in TABLE 1, as can be seen, *E*-4a and *E*-4b isomers are more stable than *Z*-4a and *Z*-4b forms (0.69 and 1.10 kcal/mol, respectively) at B3LYP level of theory.

TABLE 1 : The relative energy (kcal/mol) for both the *Z*- and *E*- isomers of ylides 4a and 4b, obtained at HF/6-31G (d,p) and B3LYP/6-311++G(d,p) levels.

Geometrical isomer	HF	B3LYP
Z-4a	1.23	0.69
E-4a	0.00	0.00
Z-4b	1.24	1.10
E-4b	0.00	0.00

Further investigation was undertaken in order to determine more effective factors on stability of the two *Z*- and *E*- isomers on the basis of AIM calculations at HF/6-31G(d,p) level of theory by the AIM2000 program package[33]. In recent years, AIM theory has often applied in the analysis of H-bonds. In this theory, the topological properties of the electron density distribution are derived from the gradient vector field of the electron density $\nabla\rho(r)$ and on the Laplacian of the electron density $\nabla^2\rho(r)$. The Laplacian of the electron density, $\nabla^2\rho(r)$, identifies regions of space wherein the electronic charge is locally depleted [$\nabla^2\rho(r) > 0$] or built up [$\nabla^2\rho(r) < 0$][32]. Two interacting atoms in a molecule form a critical point in the electron density, where $\nabla\rho(r) = 0$, called the bond critical point (BCP). The values of the charge density and its Laplacian at these critical points give useful information regarding the strength of the H-bonds[33]. The ranges of $\rho(r)$ and $^2\rho(r)$ are 0.002 – 0.035 e/a_0^3 and 0.024 – 0.139 e/a_0^5, respectively, if H-bonds exist[34]. The AIM calculation indicates intramolecular hydrogen bond critical points (H-BCP) for the two *Z*-4(a, b) and *E*-4(a, b) isomers. Intramolecular H-BCPs along with a part of molecular graphs for the two rotational isomers are shown in Figures 2 and 3 (dotted line). Most important geometrical parameters involving some H-bonds (bond length and their relevant bond angle) are reported in TABLE 2. The electron density $(\rho)\times10^3$, Laplacian of electron density $\nabla^2\rho(r)\times10^3$, and energy density $-H(r)\times10^4$ are also reported in TABLES 3 and 4. A negative total energy density at the BCP reflects a dominance of potential energy density, which is the consequence of accumulated stabilizing electronic charge[35]. Herein, the number of hydrogen bonds in both categories (*E*-4a and *Z*-4a) and (*E*-4b and *Z*-4b) are (5 and 5) and also (6 and 5) respectively. The values of ρ and $\nabla^2\rho(r)\times10^3$ for those are in the ranges (0.008 – 0.013 and 0.008 – 0.011 e/a_0^3) and (0.0009 – 0.013 and 0.008 – 0.011 e/a_0^3) and also (30.28 – 48.44 and 31.23 – 45.54 e/a_0^5) and (3.16 – 48.38 and 31.40 – 42.43 e/a_0^5), respectively. In addition, the Hamiltonian $[-H(r)\times10^4]$ are in the ranges (6.37 – 17.82 and 5.95 – 17.98 au) and (2.08 – 17.82 and 5.88 – 17.92 au), respectively (See TABLES 3 and 4). These HBs show $\nabla^2\rho(r) > 0$ and $H(r) < 0$, which according to classification of Rozas et al.[36] are medium-strength hydrogen bonds. In both ylides the dipole moment for the two *E*-4a and *E*-4b isomers (2.94 and 2.88 D) are smaller than the two *Z*-4a and *Z*-4b isomers (5.61 and 5.41 D, respectively) and the value of $-H_{tot}$ $(=\sum -H(r)\times10^4)$ for the two *E*-4a and *E*-4b isomers (63.72 and 65.85 au) are smaller than the two *Z*-4a *and Z*-4b isomers (67.37 and 67.44 au, respectively). Although, $-H_{tot}$ in both the *E*-4(a, b) are smaller than the *Z*-4(a, b) and appear as an effective factor on instability of the *E*-4(a, b), but the values of dipole moment in the *E*-4(a, b) are smaller than *Z*-4(a, b) as an important fact on stability of *E*-4(a, b). It seems that stability on both the *E*-4(a, b) have been emerged from a result of the two opposite factors during those are just influenced the *E*-4(a, b) isomers. The results are summarized in TABLE 5. On the basis of theoretical calculations (TABLE 1), both the *E*-4a and *E*-4b have a slightly stability with respect to the two *Z*-4a and *Z*-4b (0.69 and 1.10 kcal/mol, respectively) isomers and seems to be different from the results of predictable properties of the most important geometrical parameters (TABLE 5). Perhaps, this slightly different behavior is relevant to the huge structures of the two ylides 4(a, b) involving three large atoms such as the sulfur, nitrogen and phosphorus and the large number of other atoms (C and H). This point, made a limi-

tation in application of basis set higher than B3LYP/6-311++G(d,p) in a higher performance to gain more accurate calculations. Nevertheless, the results involving a considerable difference in dipole moment as a dominate factor of stability over a small difference in total Hamiltonian ($-H_{tot}$) as a instability factor in the *E*-4(a, b) category, are compatible with the experiment results from the ^{1}H, ^{13}C, ^{31}P NMR spectroscopes[30] wich indicate the two isomers of *E*-4a and *E*-4b with the experimental abundance percentage of 69% (major forms) with respect to the *Z*-4(a, b) (minor forms).

Also, the charge on different atoms which are calculated by AIM and NPA methods and also CHelpG keyword at HF/6-31G(d,p) level are reported in TABLE 6 for the two *Z*- and *E*- isomers of ylides 4a and 4b. There is good agreement between the results in three methods.

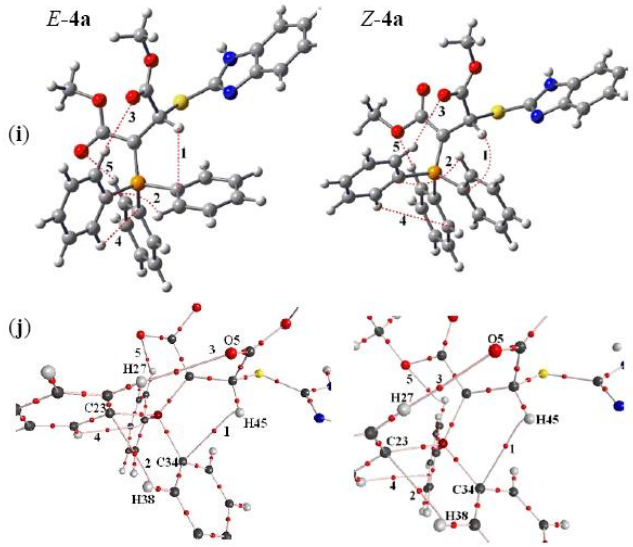

Figure 2 : (i) Intramolecular hydrogen bonds (dotted lines) in the two *E*-4a and *Z*-4a geometrical isomers of stable ylide 4a, (j) Part of molecular graphs, including intramolecular hydrogen bond critical points (BCPS) for the two rotational isomers such as *E*-4a and *Z*-4a. Small red spheres, and lines corresponding to BCPS bond paths, respectively.

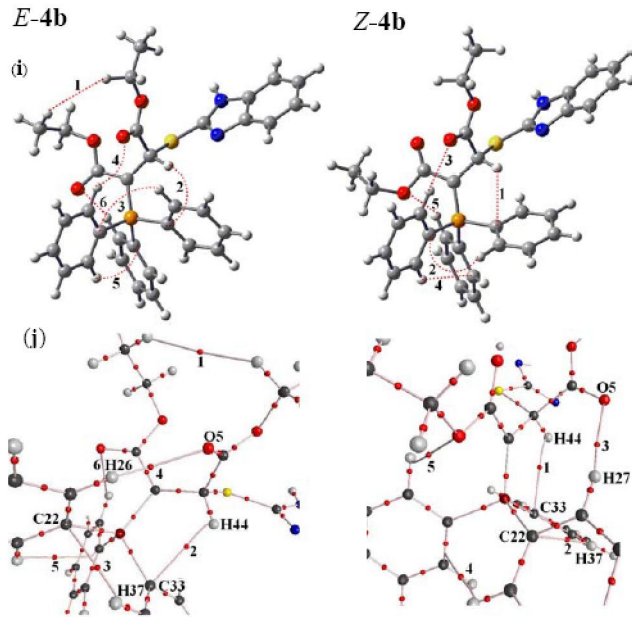

Figure 3 : (i) Intramolecular hydrogen bonds (dotted lines) in the two *E*-4b and *Z*-4b geometrical isomers of stable ylide 4b, (j) Part of molecular graphs, including intramolecular hydrogen bond critical points (BCPS) for the two rotational isomers such as *E*-4b and *Z*-4b. Small red spheres, and lines corresponding to BCPS bond paths, respectively.

TABLE 2 : Most important geometrical parameters corresponding to H-bonds (bond lengths and their relevant angles) for the two *Z* and *E* isomers in both ylides 4a and 4b. Bond lengths in Angstroms and bond angles in degrees, respectively

	E-4a	*Z*-4a	*E*-4b	*Z*-4b
$C_3H_{45}...C_{34}$	2.53[a](117.05)[b]	2.45(116.52)		
$C_{35}H_{38}...C_{23}$	2.67(108.09)	2.68(107.67)		
$O_5H27...C_{24}$	2.49(170.35)	2.47(170.02)		
$C_3H_{44}...C_{33}$			2.53(117.01)	2.54(116.59)
$C_{34}H_{37}...C_{22}$			2.67(108.09)	2.68(107.63)
$O_5H_{26}...C_{23}$			2.49(170.33)	2.46(169.82)

[a]bond length; [b]bond angle

TABLE 3 : The values of $a = \rho \times 10^3$, $b = \nabla 2\rho \times 10^3$ and $c = -H(r) \times 10^4$ for both the *Z*-4a and *E*-4a isomers of ylide 4a calculated at the hydrogen bond critical points. All quantities are in atomic units

E	a	b	c	*Z*	a	b	c
1	11.71	42.74	17.51	1	11.48	42.54	17.98
2	9.70	36.96	17.82	2	9.50	35.74	17.26
3	8.47	30.28	6.37	3	8.83	31.23	5.95
4	9.05	32.44	15.59	4	9.16	31.50	14.47
5	13.58	48.44	6.43	5	9.43	37.50	11.71

TABLE 4 : The values of $a = \rho \times 10^3$, $b = \nabla 2\rho \times 10^3$ and $c = -H(r) \times 10^4$ for both the *Z*-4b and *E*-4b isomers of ylide 4b calculated at the hydrogen bond critical points. All quantities are in atomic units

E	a	b	c	*Z*	a	b	c
1	0.93	3.16	2.08	1	11.46	42.43	17.92
2	11.67	42.58	17.47	2	9.49	35.49	17.10
3	9.69	36.96	17.82	3	8.89	31.40	5.88
4	8.47	30.28	6.38	4	9.18	31.60	14.47
5	9.03	32.32	15.54	5	9.02	36.34	12.08
6	13.54	48.38	6.57				

TABLE 5 : The most important geometrical parameters involving the value of -H_{tot}/au, dipole moment/D and the number of hydrogen bonds for the two *Z*- and *E*- isomers of ylides 4a and 4b.

Geometrical isomer	-H_{tot}/au	dipole moment/D	number of hydrogen bond
E-4a	63.72	2.94	5
Z-4a	67.37	5.61	5
E-4b	65.85	2.88	6
Z-4b	67.46	5.41	5

TABLE 6 : The charges on different atoms for the two *E* and *Z* isomers in both ylides 4a and 4b, calculated at HF/6-31G(d,p) theoretical level.

number of atom	*E*-4a	*Z*-4a	*E*-4b	*Z*-4b
C1	1.86[a] (0.96)[b]	1.87 (0.96)	1.86 (0.96)	1.87 (0.96)
	0.87[c]	0.88	0.86	0.86
C2	-0.75 (-0.88)	-0.80 (-0.89)	-0.79 (-0.88)	-0.79 (-0.89)
	-0.52	-0.45	-0.50	-0.50
C3	25 (-0.43)	25 (-0.43)	29 (-0.43)	27 (-0.42)
	0.31	0.30	0.38	0.36
O46	-1.41 (-0.80)	-1.35 (-0.76)	-1.26 (-0.66)	-1.31 (-0.67)
	-0.71	-0.65	-0.48	-0.55
O47(45)[d]	-1.27 (-0.65)	-1.28 (-0.66)	-1.40 (-0.80)	-1.38 (-0.77)
	-0.37	-0.46	-0.68	-0.62
P11(10)	3.25 (1.88)	3.25 (1.87)	3.25 (1.88)	3.25 (1.87)
	0.16	0.08	0.12	0.17

[a]Calculated by AIM method; [b]Calculated by NPA method; [c]Calculated by CHelpG keyword; [d]The numbering atoms for structure 4b are in parentheses.

Kinetics studies

To gain further insight into mechanism in reaction between triphenylphosphin 1, dialkyl acetylenedicarboxylates 2 and 2-mercaptobenzimidazole 3 (as a SH- heterocyclic compound) for generation of phosphorus ylids 4a-c, a kinetics study of the reactions was undertaken by UV spectrophotometeric technique. Synthesis of these reactions has been reported earlier[30]. To find the appropriate wavelength, in the first experiment, 3×10^{-3} M solution of compounds 1, 2c and 3 was prepared in 1, 2-dichloroethane as solvent and the relevant spectra were recorded over the wavelength range 200-400 nm. Figures 4, 5 and 6 show the ultraviolet spectra of compounds 1, 2c and 3 respectively. In a second experiment, the reaction monitored by recording scans of the entire spectra every 10 min over the whole reaction time in the presence of 1, 2c and 3 at ambient temperature as shown in Figure 7. From this, the appropriate wavelength was found to be 335 nm (corresponding mainly to product 4). The UV-vis spectra of compound 4c were measured over the concentration range (2×10^{-4}M = M_{4c} =10^{-3}M) to check for a linear relationship between absorbance values and concentrations. With the suitable concentration range and wavelength identified, the following procedure was employed.

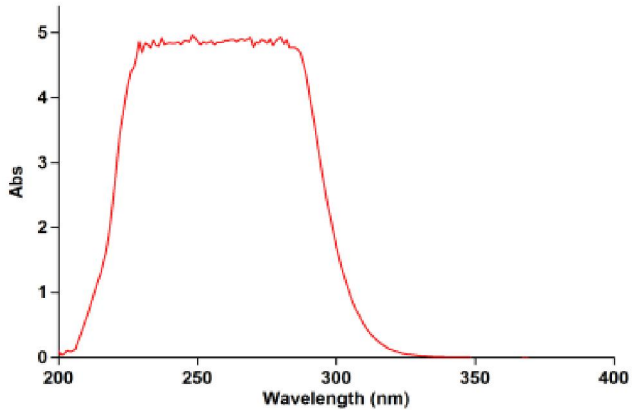

Figure 4 : The UV spectrum of 10^{-3}M triphenylphosphine 1 in 1, 2-dichloroethane

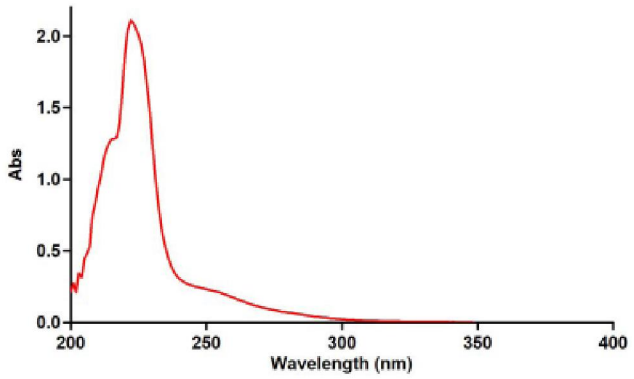

Figure 5 : The UV spectrum of 10^{-3}M di-*tert*-butyl acetylenedicarboxylate 2c in 1, 2-dichloroethane

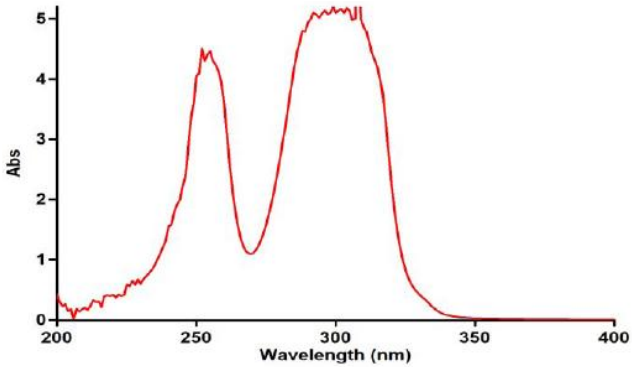

Figure 6 : The UV spectrum of 10^{-3}M 2-mercaptobenzimidazole 3 in 1, 2-dichloroethane

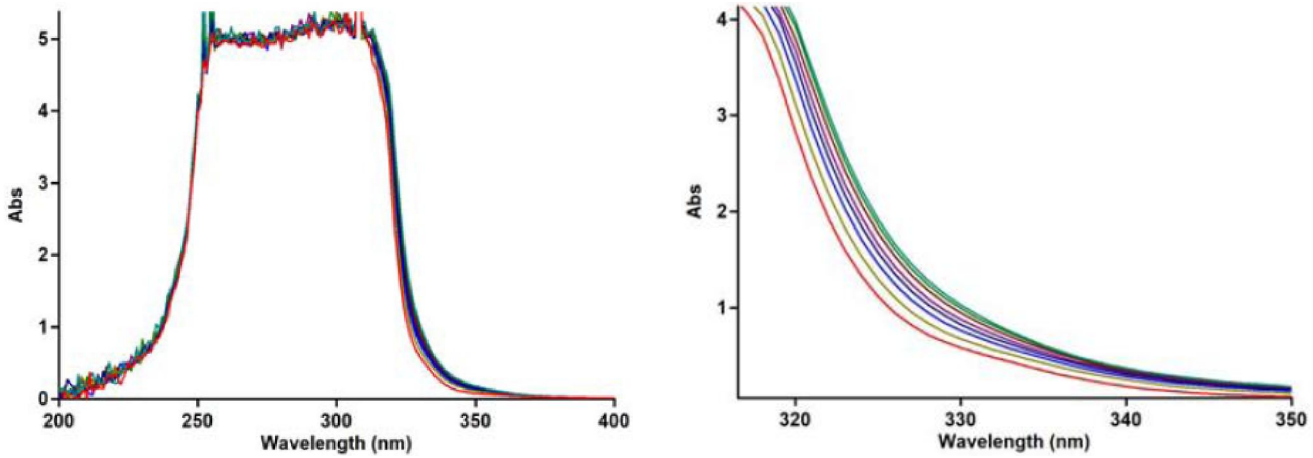

Figure 7 : (i) The UV spectra of the reaction between 1, 2c and 3 with 10^{-3}M concentration of each compound as reaction proceeds in 1, 2-dichloroethane with 10 mm light-path cell. (j) Expanded section of UV spectra over the wavelength range 315-350 nm.

For each kinetic experiment, the reaction kinetics was followed by plotting UV absorbance against time at 12.0ºC in 1, 2-dichloroethane. Figure 8 shows the absorbance change (dotted line) versus time for the 1:1:1 addition reaction between compounds 1, 2c and 3 at 12.0ºC. Using the original experimental absorbance versus time data provided a second-order fit curve (full line) by the software associated with the UV instrument[37] that fits exactly the experimental curve (dotted line) (Figure 9). This result indicates that the reaction between triphenylphosphine 1, di-*tert*-butyl acetylenedicarboxylate 2c and 3 follows second-order kinetics. The second-order rate constant (k_2) is then automatically calculated using a standard equation[37] within the program at 12.0ºC that is reported in TABLE 7.

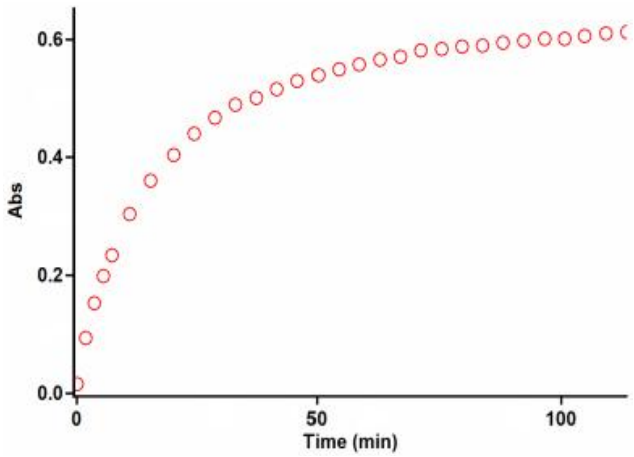

Figure 8 : The experimental absorbance changes (dotted line) against time at 335 nm for the reaction between compounds 1, 2c and 3 at 12.0 ºC in 1, 2-dichloroethane

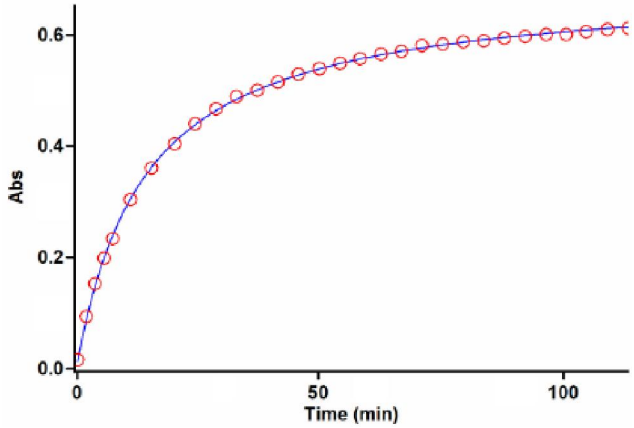

Figure 9 : Second order fit curve (full line) accompanied by the original experimental curve (dotted line) for the reaction between compounds 1, 2c and 3 at 335 nm and 12.0ºC in 1, 2-dichloroethane

Furthermore, kinetic studies were carried out in the continuation of experiments with different concentrations (5×10^{-3} M and 7×10^{-3} M) respectively. As expected, the second-order rate constant was independent of concentration and its value was the same as in the previous experiment.

Effect of solvents and temperature

To determine the effect of change in temperature and solvent environment on the rate of reaction, it was elected to perform various experiments at different temperatures and solvent polarities but otherwise under the same conditions as for the previous experiment. For this purpose, ethyl acetate with 6 dielectric constant was chosen as a suitable solvent since it is not only could be dissolved all compounds but also did not re-

act with them. The rate constant of reaction in different solvents and temperatures are given in TABLE 7. The results show that the rate of reaction in each case was increased at higher temperatures. In addition, the rate of reaction between 1, 2c and 3 was accelerated in a higher dielectric constant environment (1, 2-dichloroethane) in comparison with a lower dielectric constant environment (ethyl acetate) at all temperatures investigated. In the temperature range studied, the dependence of the second-order rate constant ($\ln k_2$) on reciprocal temperature is consistent with the Arrhenius equation (Figure 10), giving activation energy of reaction between 1, 2 and 3 from the slope (TABLE 10).

TABLE 7 : Values of overall second order rate constant for the reaction between 1, 2c and 3 in the presence of solvents such as 1, 2-dichloroethane and ethyl acetate, respectively, at all temperatures investigated.

Solvent	ε	k_2.M^{-1}.min^{-1}			
		12.0°C	17.0°C	22.0°C	27.0°C
1,2-dichloroethane	10	83.5	98.7	122.9	155.8
ethyl acetate	6	60.0	80.0	111.2	140.1

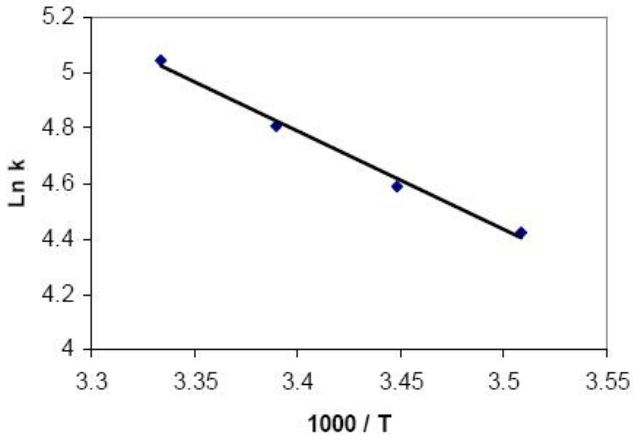

Figure 10 : Dependence of second order rate constant ($\ln k_2$) on reciprocal temperature for the reaction between compounds 1, 2c and 3 measured at wavelength 335 nm in 1, 2-dichloroethanein accordance with Arrhenius equation.

Effect of concentration

To determine reaction order with respect to triphenylphosphine 1 and dialkyl acetylenedicarboxylate 2 (2c), in the continuation of experiments, all kinetic studies were carried out in the presence of excess 3. Under this condition, the rate equation may therefore be expressed as:

$$\text{rate} = k_{obs}[1]^{\alpha}[2]^{\beta} \quad k_{obs} = k_2[3]^{\gamma} \text{ or}$$

$$\text{Ln}k_{obs} = \text{Ln}k_2 + \gamma\,\text{Ln}[3] \qquad (1)$$

In this case (3×10^{-2} M of 3 instead of 3×10^{-3} M), second order fit curve (full line) against time at 335 nm exactly fits to the original experimental absorbance versus time data. The value of rate constant was the same as that of obtained from the previous experiment (3×10^{-3} M). Same results obtained with repetition of the experiments in 5×10^{-2}M and 7×10^{-2}M of 3. In fact, the experimental data indicated that the observed pseudo second order rate constant (k_{obs}) was equal to the second order rate constant (k_2), this is possible when γ is zero in equation (1) and the reaction is zero order with respect to 3 (as a SH-acid) and the sum of 1 and 2 (2c) ($\alpha + \beta = 2$), respectively.

To determine reaction order with respect to dialkyl acetylenedicarboxylate 2 (2c), the continuation of experiment was performed in the presence of excess of 1 (rate $= k'_{obs}[3]^{\gamma}[2]^{\beta}$, $k'_{obs} = k_2[1]^{\alpha}(2)$). The original experimental absorbance versus time data and provide a pseudo first order fit curve at 335 nm, which exactly fits the experimental curve (dotted line) as shown in Figure 11.

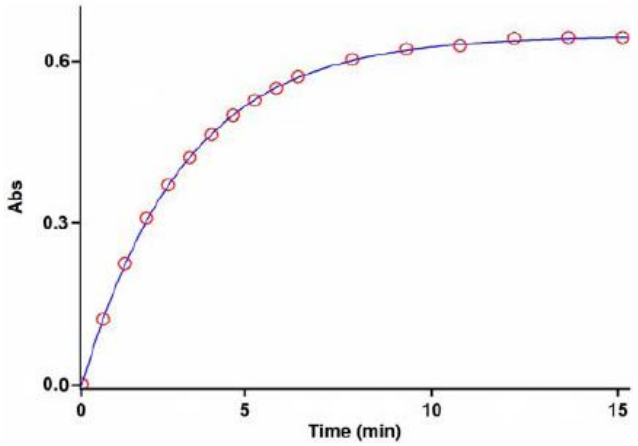

Figure 11 : Pseudo first order fit curve (full line) for the reaction between 2c and 3 in the presence of excess 1 (10^{-2}M) at 335 nm and 12.0°C in 1, 2-dichloroethane

As a result since $\gamma = 0$ (as determined previously), it is reasonable to accept that the reaction is first order with respect to compound 2 (2c) ($\beta = 1$). Because the overall order of reaction is 2 ($\alpha + \beta + \gamma = 2$) it is obvious that $\alpha = 1$ and the reaction order with respect to triphenylphosphine 1 must be equal to one. This observation was obtained also for reactions between (1, 2b and 3) and (1, 2a and 3). Based on the above results, a simplified proposed reaction mechanism is shown in Figure 12.

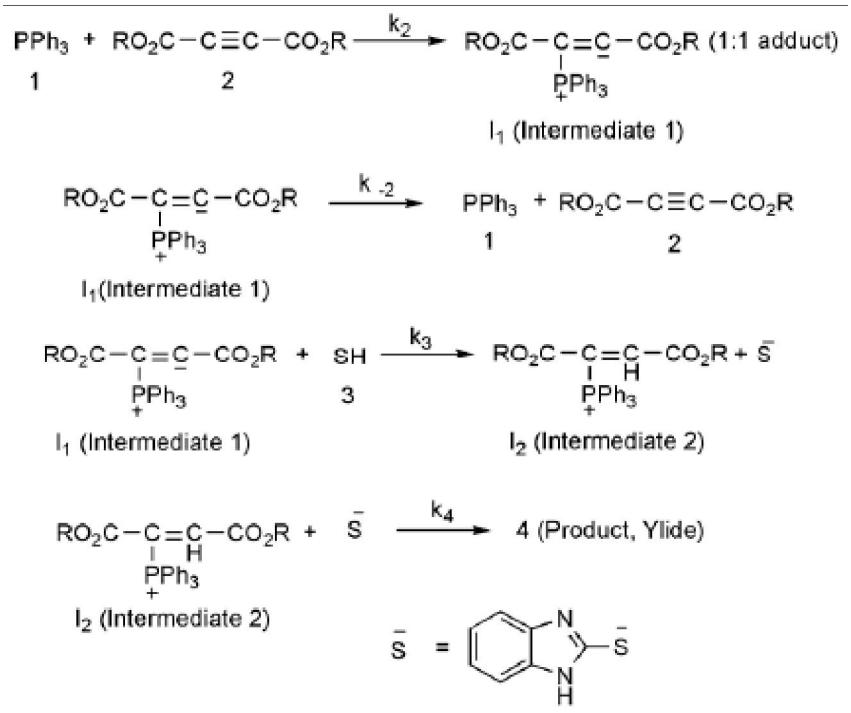

Figure 12 : Proposed mechanism for the reaction between 1, 2(2a, 2b or 2c) and 3 for generation of phosphorus ylides 4a-c.

The experimental results indicate that the third step (rate constant k_3) is possibly fast. In contrast, it may be assumed that the third step is the rate determining step for the proposed mechanism. In this case the rate law can be expressed as follows:

$$\mathbf{rate = k_3 [I_1][3]} \qquad \mathbf{(3)}$$

The steady state assumption can be employed for $[I_1]$ which is generated following equation,

$$\mathbf{[I_1]=\frac{k_2[1][2]}{k_{-2}+k_3[3]}}$$

The value of $[I_1]$ can be replaced in equation (3) to obtain this equation:

$$\mathbf{rate=\frac{k_2 k_3 [1][2][3]}{k_{-2}+k_3 [3]}}$$

Since it was assumed that k_3 is relevant to the rate determining step, it is reasonable to make the following assumption: $k_{-2} >> k_3[3]$

So the rate of low becomes: $\mathbf{rate=\frac{k_2 k_3 [1][2][3]}{k_{-2}}}$

The final equation is indicates that overall order of reaction is three which is not compatible with experimental overall order of reaction (= two). In addition, according to this equation, the order of reaction with respect to 2-mercaptobenzimidazole 3 is one whereas, it was actually shown to be equal to zero. For this reason, it appeared that the third step is fast. If we assume that the fourth step (rate constant k_4) is the rate-determining step for the proposed mechanism, in this case, there are two ionic species to consider in the rate determining step, namely phosphonium ion (I_2) and 2-mercaptobenzimidazole (S^-). The phosphonium and 2-mercaptobenzimidazole ions, as we see in Figure 12, have full positive and negative charges and form very powerful ion- dipole bonds to the 1, 2-dichloroethane, the high dielectric constant solvent. However, the transition state for the reaction between two ions carries a dispersed charge, which here is divided between the attacking 2-mercaptobenzimidazole and the phosphonium ions. Bonding of solvent (1, 2-dichloroethane) to this dispersed charge would be much weaker than to the concentrated charge of 2-mercaptobenzimidazole and phosphonium ions. The solvent thus stabilize the species ions more than it would the transition state, and therefore E_a would be higher, slowing down the reaction. However, in practice, 1, 2-dichloroethane speeds up the reaction and for this reason, the fourth

step, which is independent of the change in the solvent medium, could not be the rate determining step. Furthermore, the rate law of formation of the product (fourth step) for a proposed reaction mechanism with application of steady state assumption can be expressed by:

$$\mathbf{rate} = k_4[I_2][S^-]$$

By application of steady state for $[I_2]$ and $[S^-]$, and replacement of their values in the above equation, the following equation is obtained:

$$\mathbf{rate} = \frac{k_2 k_3 [1][2][3]}{k_{-2} + k_3[3]} \quad (4)$$

This equation is independent of rate constant for the fourth step (k_4) and shows why the fourth step would not be affected by a change in the solvent medium. In addition, it has been suggested earlier that the kinetics of ionic species' phenomena (e.g., the fourth step) are very fast[38]. If the first step (rate constant k_2) were the rate determining step, in this case, two reactants (triphenylphosphine 1 and dialkyl acetylenedicarboxylate 2), as we see in Figure 12, have no charge and could not form strong ion-dipole bonds to the high dielectric constant solvent, 1,2-dichloroethane. However, the transition state carries a dispersed charge which here is divided between the attacking 1 and 2 and, hence, bonding of solvent to this dispersed charge is much stronger than the reactants, which lack charge. The solvent thus stabilizes the transition state more than it does the reactants and, therefore, E_a is reduced which speeds up the reaction. Our experimental results show that the solvent with higher dielectric constant exerts a power full effect on the rate of reaction (in fact, the first step has rate constant k_2 in the proposed mechanism) but the opposite occurs with the solvent of lower dielectric constant, (see TABLES 7, 8 and 9). The results of the current work (effects of solvent and concentration of compounds) have provided useful evidence for steps 1 (k_2), 3 (k_3) and 4 (k_4) of the reactions between triphenylphosphine 1, dialkyl acetylenedicarboxylate 2 (2a, 2b or 2c) and 2-mercaptobenzimidazole 3. Two steps involving 3 and 4 are not determining, although the discussed effects, taken altogether, are compatible with first step (k_2) of the proposed mechanism and would allow it to be the rate-determining step. However, a good kinetic description of the experimental result using a mechanistic scheme based upon the steady state approximation is frequently taken as evidence of its validity. By application of this, the rate formation of product 4 from the reaction mechanism (Figure 12) is given by:

$$\frac{d[4]}{dt} = \frac{d[ylide]}{dt} = \mathbf{rate} = k_4[I_2][S^-] \quad (5)$$

We can apply the steady-state approximation to $[I_1]$ and $[I_2]$;

$$\frac{d[I_1]}{dt} = k_2[1][2] - k_{-2}[I_1] - k_3[I_1][3],$$

$$\frac{d[I_2]}{dt} = k_3[I_1][3] - k_4[I_2][S^-]$$

To obtain a suitable expression for $[I_2]$ to put into equation (5) we can assume that, after an initial brief period, the concentration of $[I_1]$ and $[I_2]$ achieve a steady state with their rates of formation and rates of disappearance just balanced. Therefore $\frac{d[I_1]}{dt}$ and $\frac{d[I_2]}{dt}$ are zero and we can obtain expressions for $[I_2]$ and $[I_1]$ as follows:

$$\frac{d[I_2]}{dt} = 0, \quad [I_2] = \frac{k_3[I_1][3]}{k_4[S^-]} \quad (6)$$

$$\frac{d[I_1]}{dt} = 0, \quad [I_1] = \frac{k_2[1][2]}{k_{-2} + k_3[3]} \quad (7)$$

We can now replace $[I_1]$ in the equation (6) to obtain this equation:

$$[I_2] = \frac{k_2 k_3 [1][2][3]}{k_4[S^-]\left[k_{-2} + k_3[3]\right]}$$

The value of $[I_2]$ can be put into equation (5) to obtain the rate equation (8) for proposed mechanism:

$$\mathbf{rate} = \frac{k_2 k_3 k_4 [1][2][3][S^-]}{k_4[S^-]\left[k_{-2} + k_3[3]\right]} \quad \mathbf{or} \quad \mathbf{rate} = \frac{k_2 k_3 [1][2][3]}{\left[k_{-2} + k_3[3]\right]} \quad (8)$$

Since experimental data were indicated that steps 3 (k_3) and 4 (k_4) are fast but step 1 (k_2) is slow, it is therefore reasonable to make the following assumption:

$$k_3[3] >> k_{-2}$$

So the rate equation becomes:

$$\mathbf{rate} = k_2[1][2] \quad (9)$$

This equation which was obtained from a mechanistic scheme (shown in Figure 12) by applying the steady-state approximation is compatible with the results ob-

tained by UV spectrophotometery. With respect to the equation (9) that is shown overall reaction rate (Figure 1), the activation parameters involving $\Delta G^{\#}$, $\Delta S^{\#}$ and $\Delta H^{\#}$ for three reactions (1, 2a and 3), (1, 2b and 3) and also (1, 2c and 3) could be now calculated by Eyring equation for the first step (rate determining step), as an elementary reaction, the results are reported in TABLE 10.

Further kinetic investigations

Effect of structure of dialkyl acetylenedicarboxylates

To confirm the above observations, further experiments were performed with diethyl acetylenedicarboxylate 2b and dimethyl acetylenedicarboxylate 2a, respectively, under the same conditions used in the previous experiments. The values of the second-order rate constant (k_2) for the reactions between (1, 2b and 3) and (1, 2a and 3) are reported in TABLES 8 and 9, respectively for all solvents and temperatures investigated. The original experimental absorbance curves (dotted line) accompanied by the second order fit curves (full line), which exactly fit experimental curves (dotted line) (Figures 13 and 14) confirm the previous observations again for both reactions at 12.0ºC and 335 nm.

As can be seen from TABLES 8 and 9 the behavior of diethyl acetylenedicarboxylate 2b and dimethyl acetylenedicarboxylate 2a is the same as for the di-*tert*-butyl acetylenedicarboxylate 2c (TABLE 7) with respect to the reaction with triphenylphosphine 1 and 2-mercaptobenzimidazole 3. The rate of the former reactions was also accelerated in a higher dielectric constant environment and with higher temperatures; however, these rates under the same condition are approximately 6.5 to 8.5 times more than for the reaction in the presence of di-*tert*-butyl acetylenedicarboxylate 2c (see TABLES 7, 8 and 9).

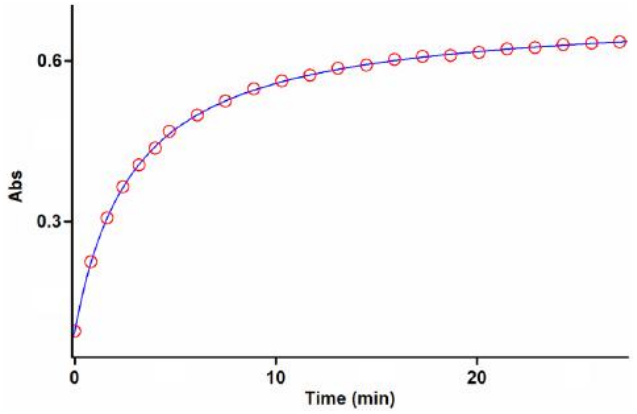

Figure 13 : Second order fit curve (full line) accompanied by the original experimental curve (dotted line) for the reaction between compounds 1, 2b and 3 at 335 nm and 12.0ºC in 1, 2-dichloroethane

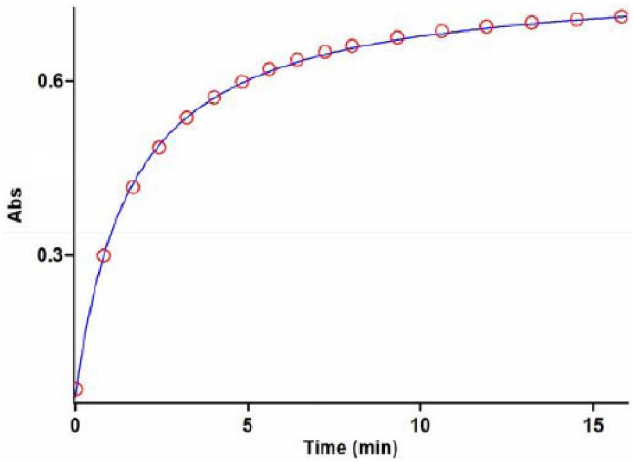

Figure 14 : Second order fit curve (full line) accompanied by the original experimental curve (dotted line) for the reaction between compounds 1, 2a and 3 at 335 nm and 12.0ºC in 1, 2-dichloroethane

TABLE 8 : Values of overall second order rate constant for the reaction between 1, 2b and 3 in the presence of solvents such as 1, 2-dichloroethane and ethyl acetate, respectively, at all temperatures investigated.

Solvent	ε	$k_2.M^{-1}.min^{-1}$			
		12.0ºC	17.0ºC	22.0ºC	27.0ºC
1,2-dichloroethane	10	531.2	592.6	670.1	776.3
ethyl acetate	6	378.1	468.0	563.4	627.4

TABLE 9 : Values of overall second order rate constant for the reaction between 1, 2a and 3 in the presence of solvents such as 1, 2-dichloroethane and ethyl acetate, respectively, at all temperatures investigated.

Solvent	ε	$k_2.M^{-1}.min^{-1}$			
		12.0ºC	17.0ºC	22.0ºC	27.0ºC
1,2-dichloroethane	10	699.2	758.1	831.1	935.6
ethyl acetate	6	580.4	699.0	790.1	925.3

TABLE 10 : The activation parameters involving ΔG#, ΔS# and ΔH# for the reactions between (1, 2a and 3), (1, 2b and 3) and (1, 2c and 3) at 12.0ºC in 1, 2-dicholoroethane on the basis of Eyring equation.

Reactions	$\Delta G^{\#}$(kJ.mol^{-1})	$\Delta H^{\#}$(kJ.mol^{-1})	$\Delta S^{\#}$(J.mol^{-1}.K^{-1})
1, 2a and 3	100.80	8.90	-321.90
1, 2b and 3	101.40	13.20	-309.50
1, 2c and 3	105.80	24.90	-283.40

It seems that both inductive and steric factors for the bulky alkyl groups in 2c tend to reduce the overall reaction rate (see equation 9). In the case of dimetyl acetylenedicarboxylate 2a, the lower steric and inductive effects of the dimethyl groups exert a powerful effect on the rate of reaction.

CONCLUSION

The assignment of the *Z*- and *E*- isomers as a minor or major form in both the ylides 4a and 4b was undertaken by AIM and NPA methods and also CHelpG keyword. Quantum mechanical calculation was clarified how the ylides 4a and 4b exist in solution as a mixture of the two geometrical isomers. This result was in good agreement with the experimental data. In addition, kinetic investigation of the reactions was undertaken using UV spectrophotometry. The results can be summarized as follow: (1) the appropriate wavelengths and concentrations were determined to follow the reaction kinetics. (2) The overall reaction order followed second-order kinetics and the reaction orders with respect to triphenylphosphine, dialkyl acetylenedicarboxylate and 2-mercaptobenzimidazole were one, one and zero respectively. (3) The rates of all reactions were accelerated at higher temperatures. Under the same conditions, the activation energy for the reaction with di-*tert*-butyl acetylenedicarboxylate 2c (29.7 kJ/mol) was higher than that for the both reactions which were followed by the diethyl acetylenedicarboxylate 2b (17.9 kJ/mol) and dimethyl acetylenedicarboxylate 2a (13.7 kJ/mol) in 1,2-dichloroethane (4) The rates of all reactions were increased in solvents with higher dielectric constant and this can be related to differences in stabilization by the solvent of the reactants and the activated complex in the transition state. (5) Increased steric bulk in the alkyl groups of the dialkyl acetylenedicarboxylates, accompanied by the correspondingly greater inductive effect, reduced the overall reaction rate. (6) With respect to the experimental data, the first step in proposed mechanism recognized as a rate-determining step (k_2) and confirmed based upon the steady-state approximation. Also, the third step was identified as a fast step (k_3). (7) The activation parameters involving $\Delta G^{\#}$, $\Delta S^{\#}$ and $\Delta H^{\#}$ were reported using Eyring equation.

ACKNOWLEDGEMENTS

Authors sincerely thank the University of Sistan & Baluchestan for providing financial support of this work.

REFERENCES

[1] M.Crayson, E.J.Griffith; 'Topics in Phosphorus Chemistry', Insterscience: New York, **7**, **(1972)**.
[2] P.Laszo; 'Organic Reaction: Simplicity and Logic', Wiley: New York, **(1995)**.
[3] A.W.Johnson; 'Ylide Chemistry', Academic Press: London, **(1966)**.
[4] J.I.G.Cadogan; 'Organophosphorus Reagent in Organic Synthesis', Academic Press: New York, **(1979)**.
[5] R.Engel; 'Synthesis of Carbon-Phosphorus Bonds', CRC Press: Boca Rotan, FL, **(1988)**.
[6] H.R.Hudson; 'Primary, Secondary and Tertiary Phosphines, Plyphosphines and Heterocyclic Organophosphorus (III) Compounds, in the Chemistry of Organophosphorus Compounds', F.R.Hantley, (Ed); Wiley: New York, **1**, 386-472 **(1990)**.
[7] D.E.C.Corbridge; 'Phosphorus: An Outline of Chemistry, Biochemistry and Uses', 5th Edition, Elsevier, Amsterdam, Holland, **(1995)**.
[8] M.T.Maghsoodlou, N.Hazeri, S.M.Habibi-Khorassani, Z.Moeeni, Gh.Marandi, M.Lashkari, M.Ghasemzadeh, H.R.Bijanzadeh; J.Chem.Res., 566 **(2007)**.
[9] A.Ramazani, A.R.Kazemizadeh, E.Ahmadi, N.Noshiranzadeh, A.Souldozi; Current Org.Chem., **12**, 59 **(2001)**.
[10] B.E.Maryanoff, A.B.Reitz; Chem.Rev., **89**, 863 **(1989)**.
[11] M.Anary-Abbasinejad, H.Anaraki-Ardakani, H.Hosseini-Mehdiabad; Phosphorus Sulfur and Silicon Ralat.Elem., **183**, 1440 **(2008)**.
[12] L.Fitjer, U.Quabeck; Synth.Commun., **15**, 855 **(1985)**.
[13] A.Hassanabadi, M.Anary-Abbasinejad, A.Dehghan; Synth.Commun., **39**, 132 **(2009)**.
[14] H.Anaraki-Ardakani, Sh.Sadeghian, F.Rastegari, A.Hassanabadi, M.Anary-Abbasinejad; Synth. Commun., **38**, 1990 **(2008)**.
[15] M.R.Islami, Z.Hassani, K.Saidi; Synth.Commun., **33**, 65 **(2003)**.
[16] A.Ramazani, A.Souldozi; Phosphorus Sulfur Silicon Relat.Elem., **180**, 2801 **(2005)**.

Full Paper

[17] I.Yavari, M.Adib, F.Jahani-Mogaddam, M.H.Sayahi; Phosphorus Sulfur and Silicon Ralat.Elem., **177**, 545 **(2002)**.
[18] M.Adib, M.Mostofi, K.Ghanbary, H.R.Bijanzadeh; Synthesis., **10**, 1663 **(2005)**.
[19] M.R.Islami, F.Mollazehi, A.Badiei, H.Sheibani; Arkivoc., **15**, 25 **(2005)**.
[20] M.T.Maghsoodlou, N.Hazeri, S.M.Habibi-Khorassani, A.Ghulame-Shahzadeh, M.Nassiri; Phosphorus Sulfur and Silicon Relat.Elem., **181**, 913 **(2006)**.
[21] I.Yavari, A.A.Alizadeh; Monatsh.Chem., **134**, 435 **(2003)**.
[22] M.Kalantari, M.R.Islami, Z.Hassani, K.Saidi; Arkivoc., **10**, 55 **(2006)**.
[23] A.Ramazani, A.Bodaghi; Tetrahedron Lett., **41**, 567 **(2000)**.
[24] I.Yavari, L.Ahmadian-Rezlighi; Phosphorus Sulfur and Silicon Relat.Elem., **181**, 771 **(2006)**.
[25] G.Keglevich, Z.Baan, I.Hermecz; Current Org. Chem., **11**, 107 **(2007)**.
[26] M.T.Maghsoodlou, S.M.Habibi-Khorassani, M.K.Rofouei, S.R.Adhamdoust, M.Nassiri; Arkivoc., **12**, 145 **(2006)**.
[27] M.A.Kazemian, M.Nassiri, A.Ebrahimi, M.T.Maghsoodlou, S.M.Habibi-Khorassani; Arkivoc., **17**, 173 **(2008)**.
[28] S.M.Habibi-Khorassani, M.T.Maghsoodlou, M.Nassiri, M.Zakarianejad, M.Fattahi; Arkivoc., **16**, 168 **(2006)**.
[29] S.M.Habibi-Khorassani, M.T.Maghsoodlou, A.Ebrahimi, M.Zakarianejad, M.Fattahi; J.Solution Chem., **36**, 1117 **(2007)**.
[30] M.T.Maghsoodlou, R.Heydari, S.M.Habibi-Khorassani, M.K.Rofouei, M.Nassiri, E.Mosaddegh, A.Hassankhani; J.Sulfur Chemistry, **27**, 341 **(2006)**.
[31] M.J.Frisch, et al.; Gaussian 98, Revision A. 7, Gaussian, Inc., Pittsburgh, PA, **(1998)**.
[32] R.F.W.Bader; Atoms in Molecules A Quantum Theory, Oxford University, New York, **(1990)**.
[33] F.W.Biegler König, J.Schönbohm, D.Bayles; J.Comput.Chem., **22**, 545 **(2001)**.
[34] S.J.Grabowski; J.Mol.Struct., **562**, 137 **(2001)**.
[35] W.D.Arnold, E.Oldfield; J.Am.Chem.Soc., **122**, 12835 **(2000)**.
[36] I.Rozas, I.Alkorta, J.Elguero; J.Am.Chem.Soc., **122**, 11154 **(2000)**.
[37] L.M.Schwartz, R.I.Gelb; Anal.Chem., **50**, 1592 **(1978)**.
[38] T.Okubo, Y.Maeda, H.Kitano; J.Phys.Che., **93**, 3721 **(1989)**.